J. Membrane Biol. 127, 9–19 (1992)

The Journal of
Membrane Biology


# Slow Voltage Inactivation of $Ca^{2+}$ Currents and Bursting Mechanisms for the Mouse Pancreatic Beta-Cell

Paul Smolen† and Joel Keizer‡

†National Institutes of Health, National Institute of Diabetes and Digestive and Kidney Diseases, Mathematical Research Branch, Bethesda, Maryland 20892, and ‡Institute of Theoretical Dynamics and Department of Chemistry, University of California, Davis, California 95616

**Summary.** Recent whole-cell electrophysiological data concerning the properties of the $Ca^{2+}$ currents in mouse $\beta$-cells are fitted by a two-current model of $Ca^{2+}$ channel kinetics. When the $\beta$-cell $K^+$ currents are added to this model, only large modifications of the measured $Ca^{2+}$ currents will reproduce the bursting pattern normally observed in mouse islets. However, when the measured $Ca^{2+}$ currents are modified only slightly and used in conjunction with a $K^+$ conductance that can be modulated dynamically by ATP concentration, reasonable bursting is obtained. Under these conditions it is the K-ATP conductance, rather than the slow voltage inactivation of the $Ca^{2+}$ current, that determines the interburst interval. We find that this latter model can be reconciled with experiments that limit the possible periodic variation of the K-ATP conductance and with recent observations of intracellular $Ca^{2+}$ bursting in islets.

**Key Words** beta-cell · bursting · calcium inactivation · voltage inactivation · K-ATP channel · insulin secretion

## Introduction

When stimulated with glucose, pancreatic $\beta$-cells exhibit repetitive, bursting electrical activity (Atwater et al., 1980). The biophysical mechanism underlying this behavior is currently under intense investigation by both experimentalists (Misler et al., 1986, 1989; Rorsman & Trube, 1986; Satin & Cook, 1988, 1989; Ashcroft & Rorsman, 1989; Cook & Ikeuchi, 1989; Valdeolmillos et al., 1989; Henquin, 1990*a*; Hopkins, Satin & Cook, 1991) and theorists (Chay & Keizer, 1983; Sherman, Rinzel & Keizer, 1988; Keizer & Magnus, 1989; Chay, 1990). While it is generally agreed that voltage-gated $Ca^{2+}$ and $K^+$ channels are responsible for rapid spikes during the active phase of a burst (Ashcroft & Rorsman, 1989), the mechanisms involved in setting the interburst interval remain unclear. Pharmacological evidence (Henquin, 1990*b*; Fatherazi & Cook, 1991; Kukuljan, Goncalves & Atwater, 1991) seems to rule out participation of $Ca^{2+}$-activated $K^+$ channels, while electrophysiological measurements on single cells suggest that ATP-sensitive $K^+$ channels may not have pacemaker activity (Smith, Ashcroft & Rorsman, 1990). Recently we have explored a mechanism for control of the interburst interval proposed by Satin and Cook (1989) that involves slow voltage inactivation of a $Ca^{2+}$ conductance (Keizer & Smolen, 1991).

Here we extend our theoretical work to analyze their recent measurements on mouse $\beta$-cells (Hopkins et al., 1991). We find that the slow voltage inactivation of mouse $\beta$-cells is sufficient to produce bursting only when the measured properties of the $Ca^{2+}$ currents are modified significantly. On the other hand, we find that slow voltage inactivation, in combination with dynamic modulation of the ATP-sensitive $K^+$ conductance, can reproduce bursting while maintaining consistency with the experiments of Smith et al. (1990). Finally, we show that this mechanism gives rise to oscillations in cytosolic $Ca^{2+}$ that resemble recent observations in pancreatic islets (Santos et al., 1991).

## Fitting $Ca^{2+}$ Currents of the Mouse $\beta$ Cell

The experiments of Hopkins et al. (1991) are consistent with two types of $Ca^{2+}$ currents, similar to those that we have modeled in HIT cells (Keizer & Smolen, 1991). In this section we develop a model of $Ca^{2+}$ currents in the mouse cell and use the published data of Hopkins et al. (1991) to generate the necessary parameters. As before, we assume a Goldman-Hodgkin-Katz form for the current-voltage relation of a single open channel, $i(V)$

$$i(V) = \mathrm{Ca}_o V \left\{ \frac{1}{1 - \exp\left[\frac{2FV}{RT}\right]} \right\} \quad (1)$$

where $V$ is the membrane potential in mV, $RT/F$ is the thermal voltage, and $\mathrm{Ca}_o$ is the external $Ca^{2+}$ concentration in mM. For the whole-cell $Ca^{2+}$ current in $fA$, we then have

$$I_{\mathrm{Ca}} = g_{\mathrm{Ca}}\, i(V) \quad (2)$$

where $g_{\mathrm{Ca}}$ is a whole-cell $Ca^{2+}$ conductance in pS $\mathrm{mM}^{-1}$. To account for two types of currents we divide the whole-cell conductance into two components as

$$g_{\mathrm{Ca}} = \bar{g}_{\mathrm{Ca}} [X_f P_O + m_s^{\infty} J (1 - X_f)]. \quad (3)$$

Here the first term represents the "fast" (ca. 100 msec) $Ca^{2+}$-inactivated $Ca^{2+}$ current that carries a fraction, $X_f$, of the maximal total conductance, $\bar{g}_{\mathrm{Ca}}$. $P_O$ denotes the fraction of fast channels that are open. The second term represents the "slow" (ca. 10 sec) voltage-inactivated $Ca^{2+}$ current. The voltage-dependent activation of the slow channels is denoted by $m_s^{\infty}(V)$, and $J$ denotes the fraction of slow channels not inactivated. As previously, we use Boltzmann-type expressions for the equilibrium values of voltage-dependent activation and inactivation (Keizer & Smolen, 1991). $J$ relaxes to its steady-state value, $J_{\infty}$, with a relaxation time $\tau_J$ whose minimum value is $T_J^*$. Explicitly,

$$m_s^{\infty}(V) = \frac{1}{\left(1 + \exp\left[\frac{(V_{ms} - V)}{S_{ms}}\right]\right)} \quad (4)$$

$$\frac{dJ}{dt} = -\frac{(J - J_{\infty})}{\tau_J} \quad (5)$$

$$\tau_J(V) = \frac{T_J}{\left\{\exp\left[\frac{(V - V_J)}{2S_J}\right] - \exp\left[\frac{-(V - V_J)}{2S_J}\right]\right\}} + T_J^* \quad (6)$$

$$J_{\infty}(V) = \frac{1}{\left(1 + \exp\left[\frac{(V - V_J)}{S_J}\right]\right)}. \quad (7)$$

Sherman, Keizer and Rinzel (1990) have developed a domain $Ca^{2+}$ model to describe $Ca^{2+}$-dependent inactivation of $Ca^{2+}$ channels in mouse $\beta$-cells (Plant, 1988). We use a variant of this model to describe the fast $Ca^{2+}$ channels. The relevant kinetic scheme is

$$C \underset{k_{-1}}{\overset{k_{+1}}{\rightleftharpoons}} O \underset{k_{-2}}{\overset{k_{+2}\mathrm{Ca}_d(V)}{\rightleftharpoons}} O\text{-Ca} \underset{k_{-3}}{\overset{k_{+3}}{\rightleftharpoons}} B. \quad (8)$$

Here $C$ is a closed state, $O$ is open, and $O$-Ca is open with $Ca^{2+}$ bound from a localized "domain" of $Ca^{2+}$ concentration, $\mathrm{Ca}_d(V)$, which is predicted to accumulate in a small region several tenths of a micrometer across around the mouth of an open channel. $B$ is a nonconducting state that is blocked by a conformational change subsequent to binding. The rate parameters, $k_{+1}$ and $k_{-1}$, can be determined from the Boltzmann-type expression for the equilibrium value of voltage-dependent activation,

$$m_f^{\infty}(V) = \frac{k_{+1}}{(k_{-1} + k_{+1})} = \frac{1}{\left(1 + \exp\left[\frac{(V_{mf} - V)}{S_{mf}}\right]\right)} \quad (9)$$

and the voltage-independent relaxation time constant for relaxation of the activation to equilibrium,

$$\tau_{mf} = \frac{1}{k_{+1} + k_{-1}}. \quad (10)$$

As Sherman et al. (1990) discuss, $\mathrm{Ca}_d(V)$ is proportional to the single-channel current-voltage relation in Eq. (1), i.e.,

$$k_{+2}\,\mathrm{Ca}_d(V) = -A\, i(V). \quad (11)$$

To simplify the kinetic scheme, the binding of $Ca^{2+}$ to the open state is assumed so rapid that the fraction of open channels with $Ca^{2+}$ bound is at steady state

$$\frac{O\text{-Ca}}{O + O\text{-Ca}} = \frac{k_{+2}\mathrm{Ca}_d(V)}{k_{+2}\mathrm{Ca}_d(V) + k_{-2}}. \quad (12)$$

The quantity $(O + O\text{-Ca})$ is $P_O$, the fraction of channels open. The dynamics of fast $Ca^{2+}$ channels are then completely described by two differential equations

$$\frac{dC}{dt} = P_O \left[\frac{k_{-2}}{k_{+2}\mathrm{Ca}_d(V) + k_{-2}}\right] k_{-1} - k_{+1} C \quad (13)$$

$$\frac{dB}{dt} = P_O \left[\frac{k_{+2}\mathrm{Ca}_d(V)}{k_{+2}\mathrm{Ca}_d(V) + k_{-2}}\right] k_{+3} - k_{-3} B \quad (14)$$

along with the relation $C + P_O + B = 1$. The equations must be solved in conjunction with the differential equation for the slow inactivation, Eq. (5), and that for the membrane potential

$$C_m \frac{dV}{dt} = -I_{Ca} \tag{15}$$

where $C_m$ is the whole-cell capacitance (5.31 pF), to obtain the dynamics of $Ca^{2+}$ currents in the $\beta$-cell.

In order to compare the predictions of this model with experiment we have simulated the protocols of Hopkins et al. (1991) by numerical integration of Eqs. (5) and (13)–(15). Hopkins et al. (1991) obtain a whole-cell current *vs.* voltage (*I-V*) curve for the mouse cells by abruptly depolarizing from a −100-mV holding potential to various membrane potentials and recording the peak current, which is elicited at the start of the depolarization. They consistently observed that the peak current declined from about −10 pA at −40 mV to essentially 0 pA at −50 mV. We term this the "*sharp threshold*" of the $Ca^{2+}$ current. We note that this sharp threshold is also seen in *I-V* curves obtained earlier by Rorsman and Trube (1986), although the earlier curve is shifted about 15 mV negative. This shift may be due to the use of the impermeant cation N-methyl-D-glucamine by Rorsman and Trube (1986), which is known to produce a negative shift in the threshold of $Ca^{2+}$ currents in heart cells (Malecot, Feindt & Trautwein, 1988).

These peak whole-cell currents are determined by the channel activation, $m_f^\infty(V)$ and $m_s^\infty(V)$. Hopkins et al. (1991) and Rorsman and Trube (1986) present data that $\tau_{mf}$ is on the order of 1 msec. We set $\tau_{mf} = 1.3$ msec unless noted otherwise. The lower panels of Fig. 1 show two examples of the time course of $Ca^{2+}$ currents obtained by numerical integration of our model after stepping the potential from −100 to −20 and 0 mV. The resulting peak *I-V* curve in Fig. 1 (filled circles) resembles the experimental curve in magnitude and shape, including the rather sharp threshold at about −40 mV. Figure 1 also shows the calculated peak *I-V* curve in which a 300-msec "prepulse" to 0 mV precedes steps to the test potentials (inverted triangles). The differences between the *I-V* curves with and without the prepulse are similar to those measured by Hopkins et al. (1991) (*cf.* their Fig. 4). We should note that the slopes of our activation curves are much steeper than those determined by Rorsman and Trube (1986) from tail currents; however, it does not appear possible to construct *I-V* curves resembling experimental data using shallower activation curves.

Hopkins et al. (1991) utilized the 300-msec prepulse in order to eliminate the fast $Ca^{2+}$-inactivated

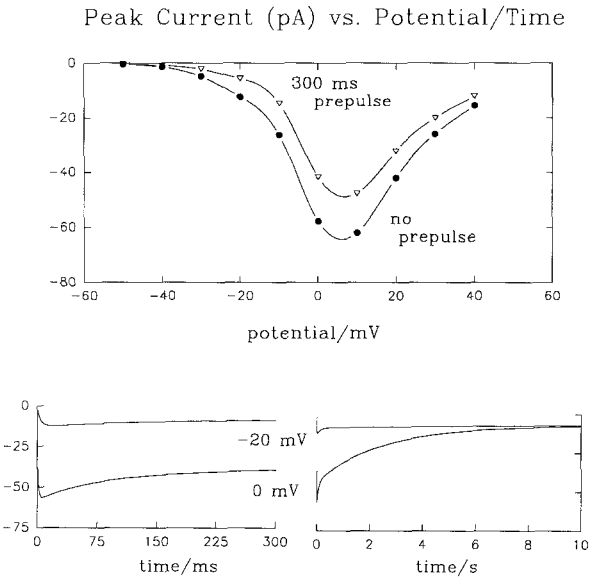


**Fig. 1.** Theoretical $Ca^{2+}$ *I-V* curves with (triangles) and without (filled circles) a 300-msec conditioning prepulse. Parameters used in these simulations are the "standard set" given in the Table, except $g_{CaG} = 0$ pS/mM.

current and, thereby, expose the slow current. They noted that this raised the sharp threshold of the *I-V* curve by approximately +15 mV. In attempting to model this shift we, therefore, set $V_{ms}$ above $V_{mf}$ and $S_{ms}$ below $S_{mf}$. Yet in order to obtain any significant shift in the threshold, we had to assume that the rate constant for the $O \rightarrow C$ transition was increased at very negative voltages, as suggested by $Ca^{2+}$ tail currents (Rorsman & Trube, 1986). Thus during the step to −100 mV that separates the prepulse from the test pulse we set $\tau_{mf}$ equal to the observed relaxation time for the tail currents, 0.18 msec. While this gives a shift of only ca. +5 mV, we have been unable to increase this significantly without seriously distorting the *I-V* curves. The shift can be increased by using a relatively large value of $V_{ms}$; however, this has the unwanted side effect of producing a significant "shoulder," or local current maximum, in the *I-V* curve, just above the threshold (at about −20 mV). While neonatal rat $\beta$-cells (Satin & Cook, 1988) and some HIT and some mouse $\beta$-cells exhibit such a "shoulder" (Satin & Cook, 1988; D. Cook, *personal communication*), the frequency of occurence of a "shoulder" in mouse cells requires further investigation.

Hopkins et al. (1991) measured the relaxation time, $\tau_h$, of the fast $Ca^{2+}$ current after depolarizing from $V = -100$ mV to various clamped potentials. The addition of the rate-limiting conformational change, $O\text{-Ca} \leftrightarrow B$, in the fast $Ca^{2+}$ channel kinetic scheme was found necessary to account for the

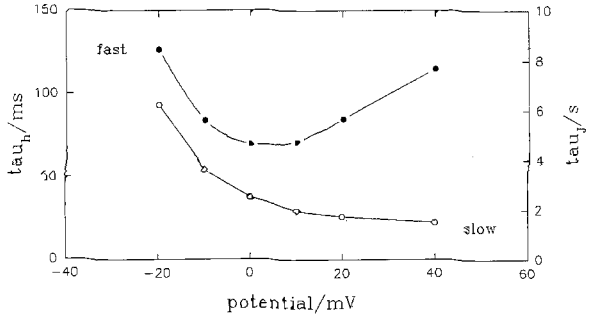


**Fig. 2.** Theoretical $Ca^{2+}$ current inactivation relaxation times for fast (filled circles, left vertical scale) and slow (open circles, right vertical scale) inactivation. Parameters are as in Fig. 1.

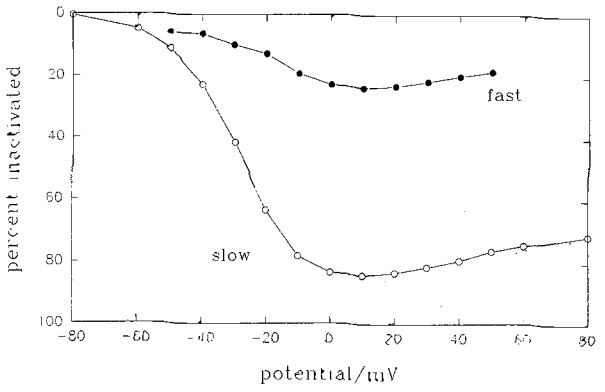


**Fig. 3.** Theoretical $Ca^{2+}$ current inactivation curves with a 100-msec (filled circles) and a 10-sec (open circles) inactivating pulse. Parameters are as in Fig. 1.

rather weak voltage dependence observed for $\tau_h$ over the range $-20$ to 10 mV. With this additional step, the following approximation, valid except at very negative or positive voltages, exists between $\tau_h$ and the equilibrium value for the fraction of channels not inactivated at a voltage $V$, denoted by $h_\infty(V)$

$$\tau_h(V) = \frac{h_\infty(V)}{k_{-3}} = \frac{1}{\left[k_{-3} + \dfrac{k_{+3}k_{+2}k_{+1}Ca_d(V)}{k_{+2}k_{+1}Ca_d(V) + k_{-2}(k_{+1} + k_{-1})}\right]} \quad (16)$$

(*cf.* Sherman et al. (1990), Eq. (8)). Thus $\tau_h$ can never be lower than $1/(k_{+3} + k_{-3})$, the value it has if no channels are in the closed state and if all open channels have $Ca^{2+}$ bound. By choosing a low value for $k_{-2}$, one can force $\tau_h$ down close to this value over a voltage range centered near 0 mV, creating a broad minimum in $\tau_h$ in agreement with experiment. Our simulations of the voltage dependence of $\tau_h$ are given in Fig. 2.

Hopkins et al. (1991) also studied fast inactivation with a three-pulse protocol, consisting of two test pulses during which peak currents are recorded, separated by a 100-msec conditioning pulse during which inactivation occurs. Our simulation of this protocol gives the upper curve in Fig. 3 for the fraction of channels inactivated as a function of the voltage $V$ of the conditioning pulse. This curve agrees with observation with the exception of two discrepancies. At very low voltages of the conditioning pulse, Hopkins et al. (1991) report virtually no inactivation, whereas we still see 5% inactivation. Since in our simulations the rate of channel recovery from inactivation is governed by $k_{-3}$, which has a voltage-independent value of 0.005 msec, this discrepancy can be explained by an increased value of $k_{-3}$ at low voltages. Above 20 mV, Hopkins et al. (1991) see a more pronounced drop in the fraction of channels inactivated than we predict. It may be that these channels are subject to a fast voltage-dependent inactivation at very positive voltages, with a fast recovery. Then fewer channels would be subject to $Ca^{2+}$ inactivation during the conditioning pulse.

Slow voltage-dependent inactivation was also studied by Hopkins et al. (1991) with comparable protocols involving a 10-sec conditioning pulse. Their data show that the relaxation time to equilibrium $\tau_J$ approaches a minimum at highly depolarized values of $V$, which is reflected by $T_J^*$ in Eq. (6). $T_J^*$ can be thought of as representing the effect of a voltage-independent kinetic step that becomes rate limiting at depolarized $V$. The lower curve in Fig. 3 gives our results for the fraction of slow channels inactivated, $1 - J$, *vs.* the voltage of a 10-sec conditioning pulse. Both this curve and the voltage dependence of the slow relaxation times, $\tau_J$, in Fig. 2 agree semi-quantitatively with the experiment. For example, the maximum inactivation occurs at the experimental value of 10 mV, where 84% of the slow current is inactivated, compared to the experimental value of about 98%. In our model this low value is due largely to the reactivation of the fast $Ca^{2+}$ channels during the interval at $-100$ mV following the second, "conditioning" pulse.

A summary of parameters for our model $Ca^{2+}$ currents that achieve the best fit to the experiments of Hopkins et al. (1991) is given in the Table. Note that in the Table, rather than an entry for $k_{+2}$, there is an entry for $A$, which is related to $k_{+2}$ through Eq. (11).

**Table.** Standard parameter values for the $\beta$-cell[a]

| | |
|---|---|
| $Ca^{2+}$ channel parameters | |
| $Ca_o = 2.5$ mM $\bar{g}_{Ca} = 2940$ pS mM$^{-1}$ | $g_{CaG} = 17.6$ pS mM$^{-1}$ |
| Fast $Ca^{2+}$ channel parameters | |
| $\tau_m = 1.3$ msec | $X_f = 0.27$ |
| $V_{mf} = -4$ mV | $S_{mf} = 6.2$ mV |
| $A = 3.024$ mM$^{-1}$ mV$^{-1}$ msec$^{-1}$ | $k_{-2} = 65$ msec$^{-1}$ |
| $k_{+3} = 0.02$ msec$^{-1}$ | $k_{-3} = 0.005$ msec$^{-1}$ |
| Slow $Ca^{2+}$ channel parameters | |
| $V_{ms} = 0$ mV | $S_{ms} = 3.6$ mV |
| $V_J = -50$ mV | $S_J = 6.3$ mV |
| $T_J = 50$ sec | $T_J^* = 1.5$ sec |
| $K^+$ channel parameters | |
| $\bar{g}_{KV} = 5000$ pS | $\bar{g}_{K\text{-}ATP} = 6000$ pS |
| $V_n = -20$ mV | $S_n = 5.3$ mV |
| $V_I = -36$ mV | $S_I = 4.5$ mV |
| $\lambda = 1.2$ | $K_1 = 0.45$ $\mu$M |
| $K_2 = 0.012$ $\mu$M | $V_K = -75$ mV |
| Parameters governing intracellular $Ca^{2+}$ and ATP dynamics: | |
| $k_{Ca} = 0.12$ msec$^{-1}$ | $\gamma = 3.61 \times 10^{-6} f A^{-1}$ $\mu$M msec$^{-1}$ |
| $f = 0.03$ | $k_a = 2.0 \times 10^{-5}$ msec$^{-1}$ |
| $R = 0.9$ | $R_1 = 0.35$ $\mu$M |
| $[A] = [ATP] + [ADP] = 1.0$ mM | |

[a] Thermal voltage $RT/F = 26.7$ mV.

## Simulation of Whole-Cell Electrical Activity

We have simulated the whole-cell electrical activity, using the calcium channel parameters derived above for mouse $\beta$-cells. To these currents we have added the important outward $K^+$ currents (Ashcroft & Rorsman, 1989). The current due to the delayed rectifier channel, $I_{KV}$, is written as follows

$$I_{KV} = \bar{g}_{KV} n I (V - V_K) \tag{17}$$

where $\bar{g}_{KV}$ is the maximal conductance, $V_K$ is the resting potential for $K^+$, $n$ is the activation, and $I$ is the inactivation. The steady-state values of $n$ and $I$ are

$$n_\infty(V) = \frac{1}{\left(1 + \exp\left[\frac{(V_n - V)}{S_n}\right]\right)} \tag{18}$$

$$I_\infty(V) = \frac{1}{\left(1 + \exp\left[\frac{(V_I - V)}{S_I}\right]\right)}. \tag{19}$$

We use values for $V_n$, $S_n$, $V_I$, and $S_I$ close to those determined by Rorsman and Trube (1986) via tail-current analysis; *cf.* the Table. These authors also give data for the relaxation time of $n$ to $n_\infty$, which enabled us to model the relaxation time constant for $n$, $\tau_n(V)$,

$$\tau_n(V) = \frac{T_N}{\lambda\left\{\exp\left[\frac{(V - V_K)}{65}\right] - \exp\left[\frac{-(V - V_K)}{20}\right]\right\}} \tag{20}$$

with $T_N = 60$ msec and $\lambda$ adjustable but on the order of unity. The differential equations describing the activation and inactivation of this channel are then

$$\frac{dn}{dt} = -\frac{(n - n_\infty)}{\tau_n} \tag{21}$$

$$\frac{dI}{dt} = -\frac{(I - I_\infty)}{\tau_I} \tag{22}$$

where $\tau_I$ is approximately 2.6 sec (Rorsman & Trube, 1986). We have added the slow inactivation of the delayed rectifier, $I$, to our calculations because it reduces the net outward current, and, therefore, tends to compensate for reduction in the outward current caused by the slow $Ca^{2+}$ channel inactivation, $J$.

In the absence of glucose the ATP-modulated $K^+$ channel, or K-ATP channel, maintains the membrane potential close to $V_K$. One effect of glucose is to reduce the whole-cell conductance, $g_{K\text{-}ATP}$, to a few hundred pS (Smith et al., 1990), thereby depolarizing the cell. We modeled the current due to this channel, $I_{K\text{-}ATP}$, as

$$I_{K\text{-}ATP} = g_{K\text{-}ATP}(V - V_K). \tag{23}$$

These two $K^+$ currents were subtracted from the right-hand side of the differential Eq. (15). In this form the whole-cell model consists of six differential equations, Eqs. (5), (13), (14), (21), (22), and the extended Eq. (15). The model was integrated numerically to establish the properties of steady-state solutions, while the "glucose-sensing" parameter $g_{K\text{-}ATP}$ was varied in the range 0–400 pS. To understand the resulting dynamics, it is helpful to view the slow variable $J$ as a parameter for the dynamics of the other variables (Keizer & Smolen, 1991). Following the scheme originally developed by Rinzel (1985), we constructed a bifurcation diagram that shows steady and oscillating solutions of the variable $V$ as a function of $1 - J$. In previous models of whole-cell electrical activity this curve is Z-shaped (Sherman et al., 1988). Both knees of this Z curve must lie within the range $0 < (1 - J) < 1$, because physiologically $1 - J$ must remain within this range. The upper and lower branches must lie at voltages characteristic of

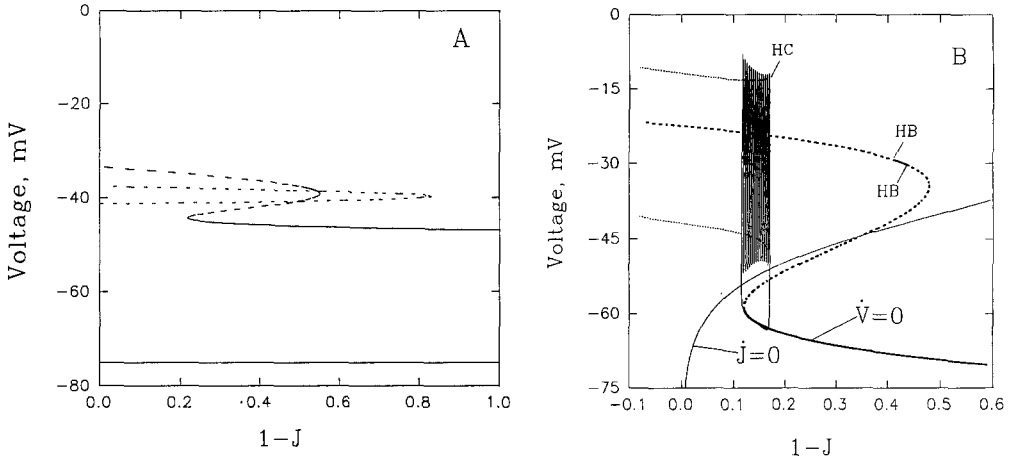


**Fig. 4.** (*A*) Z curves obtained with the slow inactivation model for mouse β-cells, with $I$ held constant at 1.0. Dotted and solid curve, obtained by shifting $V_{ms}$ and $V_{mf}$ 13 mV negative from the Table. Other $Ca^{2+}$ channel parameters are as in the Table, except $g_{CaG}$ = 0 pS mM$^{-1}$. $K^+$ channel parameters: $V_n = -19$ mV, $S_n = 5.6$ mV, $\bar{g}_{KV} = 2{,}000$ pS, $g_{K\text{-}ATP} = 167$ pS, $V_K = -75$ mV, and $\lambda = 1.2$. The dashed portion is unstable and the solid portion stable. Dashed and solid curve obtained when the voltage-insensitive $Ca^{2+}$ channel is added. Here $V_{ms}$ and $V_{mf}$ are shifted 10 mV negative from the Table, $S_{ms} = 4.6$ mV, and other $Ca^{2+}$ channel parameters are standard except $g_{CaG} = 35.3$ pS mM$^{-1}$. $K^+$ channel parameters: $V_n = -13$ mV, $S_n = 5.6$ mV, $\bar{g}_{KV} = 2{,}500$ pS, $g_{K\text{-}ATP} = 244$ pS, $V_K = -75$ mV, and $\lambda = 1.2$. The dotted curve is unstable, and the solid line is stable. (*B*) A Z curve for the HIT cell model, and superimposed burst points: Hopf bifurcation (*HB*) and homoclinic (*HC*). Solid portions are stable and dashed portions unstable (parameters as in Fig. 2*B* of Keizer and Smolen, 1991).

the active and silent phases of bursting, respectively. For standard values of $Ca^{2+}$ channel parameters (Table), there is no complete Z curve for reasonable $K^+$ channel parameters. One can only obtain a left knee (at about −70 mV), but $1 - J$ at this knee is always very negative ($-10^5$).

There is evidence that the average open time of $Ca^{2+}$ channels in the mouse β-cell increases upon exposure of the cells to glucose (Ashcroft & Smith, 1989). A modification consistent with this observation is to move $V_{ms}$ and $V_{mf}$ to more negative voltages. Previously, with $Ca^{2+}$ channel parameters determined from HIT cell data, we had been able to obtain bursts similar to experiment by shifting $V_{ms}$ and $V_{mf}$ 5 mV more negative (Keizer & Smolen, 1991). Attempting something similar, we shifted these parameters for mouse cells by up to −30 mV. With this change one can obtain complete Z curves; however, the distance between the knees is much too large. A specific example is shown in Fig. 4*A*, where both $V_{ms}$ and $V_{mf}$ have been shifted 13 mV negative of their values in the Table. The dotted curve shows the unstable right knee, and the solid line at −74 mV shows the stable hyperpolarized state. The left knee is far off scale at $1 - J = -12{,}000$. For reasonable values of $K^+$ channel parameters, small changes in the values of all other $Ca^{2+}$ channel parameters also failed to give Z curves with $0 < 1 - J < 1$.

It is the sharp lower threshold of the $Ca^{2+}$ current (at ca. −40 mV) that is responsible for the unacceptable Z curves. The reason is simply that *no amount of recovery from $Ca^{2+}$ current inactivation can have an effect at potentials where activation is almost zero*. Indeed, at the potential of the silent phase (ca. −55 mV), which is well below the sharp lower threshold, reductions in percent inactivation cannot produce sufficient inward current to depolarize the cell from the lower branch of the Z curve.

Recently, Rojas et al. (1990) have found evidence for a new class of calcium channels activated by glucose in the rat and human β-cells. We have tested the possibility that this channel might improve the Z curves based on the slow voltage inactivation, $J$. This channel can also carry other cations, so we modeled it both as a nonspecific inward leak current and as a voltage-independent calcium conductance, $I_{CaG}$

$$I_{CaG} = g_{CaG}\,Ca_o V\left\{\frac{1}{1 - \exp\left[\frac{2FV}{RT}\right]}\right\}. \tag{24}$$

As long as other parameters were chosen such that the lower threshold remained sharp, it still proved impossible to construct acceptable Z curves by adding this current to Eq. (15). One of the better results is shown as the Z-shaped curve in the center of Fig. 4*A*. Even in this case the lower and upper branches

occur in the wrong voltage range and the existence of the Z shape is extremely sensitive to parameters.

### Effect of Broadening the $Ca^{2+}$ Current Lower Threshold

In our simulations of HIT cell $Ca^{2+}$ currents (Keizer & Smolen, 1991), we chose to fit other features of the experimental measurements in preference to the sharp threshold. It is this difference that is responsible for the different Z curves and, thus, the different burst patterns in these two models. Our HIT cell simulations gave a peak $Ca^{2+}$ *I-V* curve with a broader threshold below $-40$ mV. Using parameters based on the whole HIT cell $Ca^{2+}$ current measurements of Satin and Cook (1989), supplemented with $I_{K\text{-}ATP}$ (Eq. (23)) and a delayed-rectifier current, we obtained a proper Z curve, although with anomalous bursting. Making small adjustments in the $Ca^{2+}$ activation and inactivation parameters, in a manner consistent with the experiments of Ashcroft and Smith (1989), gives the Z curve the less compact form shown in Fig. 4*B*, which supports the typical bursting pattern shown superimposed.

By broadening the threshold for the $Ca^{2+}$ currents in the mouse $\beta$-cell, our whole-cell model becomes more like that for the HIT cell. Thus one might expect modifications in the $Ca^{2+}$ currents such as increasing the activation slope factors, $S_{mf}$ and $S_{ms}$, and hyperpolarizing the half-activation voltages, $V_{mf}$ and $V_{ms}$, to give rise to bursting. An example of the type of bursting that can be obtained with these changes is shown in Fig. 5. To achieve bistability and a reasonably shaped Z curve, it was necessary to reduce the values of $V_{mf}$ and $V_{ms}$ by 4 mV from those in the Table, and to increase $S_{mf}$ and $S_{ms}$ by 3.8 mV from the values in the Table. Then these parameters have values comparable to those used to simulate HIT cell $Ca^{2+}$ currents (Keizer & Smolen, 1991). Furthermore, it was necessary to steepen significantly the slope of the steady-state slow voltage inactivation by setting $S_J$ to 2 mV. We also display in Fig. 5 the time course of [Ca], the average cytoplasmic free-$Ca^{2+}$ concentration. It is governed by the following differential equation

$$\frac{d[\mathrm{Ca}]}{dt} = f(-\gamma I_{\mathrm{Ca}} - k_{\mathrm{Ca}}[\mathrm{Ca}]). \tag{25}$$

Here $f$ is the fraction of total free cytoplasmic $Ca^{2+}$ (i.e., not bound to any macromolecule), $\gamma$ converts inward calcium current to a rate of increase of [Ca], and $k_{\mathrm{Ca}}$ is a net rate constant for efflux of $Ca^{2+}$ from the cytoplasm.

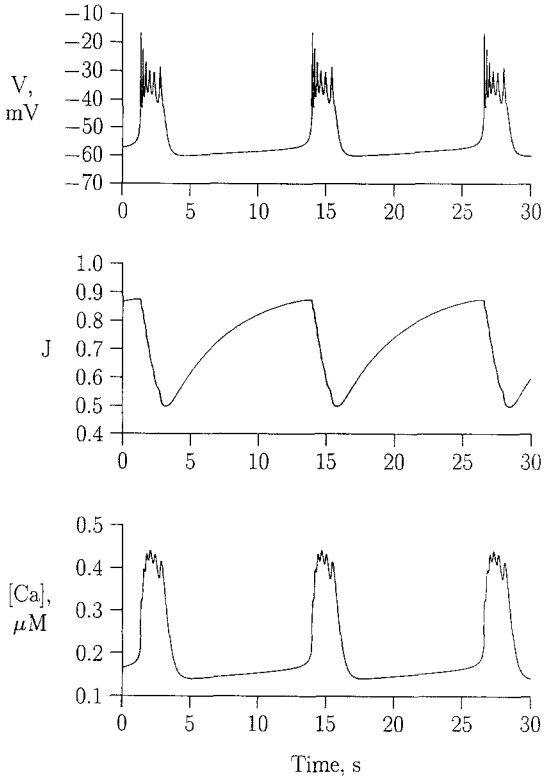


**Fig. 5.** Bursting obtained with the slow inactivation mechanism. Time courses for voltage, the slow inactivation $J$, and cytoplasmic $Ca^{2+}$ are shown. $Ca^{2+}$ channel parameters are standard except $g_{CaG} = 0$ pS mM$^{-1}$, $k_{+3} = 0.015$ msec$^{-2}$, $S_J = 2.0$ mV, and activation parameters were modified as described in the text. $K^+$ channel parameters are: $V_n = -13$ mV, $S_n = 5.3$ mV, $\bar{g}_{KV} = 2500$ pS, $g_{K\text{-}ATP} = 314$ pS, and $\lambda = 1.7$; $V_K$, $V_I$, and $S_I$ are as in the Table. The parameters for cytoplasmic $Ca^{2+}$ dynamics, $k_{Ca}$, $\gamma$, and $f$, are as in the Table. All horizontal axes are in seconds.

Analysis of the bursts in Fig. 5 confirms that they are triggered by slow voltage inactivation. For example, if the characteristic time of the slow $Ca^{2+}$ channels, $T_J$, is increased from 50 to 100 sec, there is a corresponding increase in the period of the bursts. These bursts share several features with experimental bursts in mouse $\beta$-cells, including a silent phase potential near $-55$ mV, a plateau potential near $-40$ mV and a spike amplitude on the order of 15 mV. Other features of the bursts are clearly incorrect, e.g., the spike frequency is too low (by a factor of 2–3), the spikes are overdamped, and the burst frequency is too large (by at least a factor of 2). We have not been able by any parameter manipulation to improve the spike frequency or reduce the damping. Furthermore, we find that the bursting is restricted to an extremely narrow range of values of $g_{K\text{-}ATP}$ and $\bar{g}_{Ca}$. In this sense, bursting via slow voltage inactivation is not a robust phenomenon.

According to Hopkins et al. (1991) a consider-

able proportion of $Ca^{2+}$ current is not subject to either fast or slow inactivation (*cf.* Fig. 1, lower right panel). If an additional very slow inactivation of this residual $Ca^{2+}$ current existed (especially if the "fast" $Ca^{2+}$ channels were inactivated), bursting might be obtained with less drastic parameter modifications.

### Addition of a Modulatable K-ATP Channel

Since the sharp threshold for activation of $Ca^{2+}$ currents seems difficult to reconcile with bursting via slow voltage inactivation, we have reinvestigated the notion that modulation of the conductance of K-ATP channels may contribute to bursting. Smith et al. (1990) recently have argued that modulation of this conductance does not underlie bursting. These authors obtained estimates of the input conductance in $\beta$-cells from the current responses to 10-mV voltage steps from a holding potential and concluded that the input conductance did not differ between the silent and active phases of bursting. However, the experiment could not resolve changes in the current responses of less than 0.5 pA. Given the 10-mV voltage step, 0.5 pA corresponds to a change in conductance of 50 pS. Such a conductance change is in excess of 10% of the input conductance these authors report for glucose-stimulated $\beta$-cells, 360 pS. In the original model with a modulatable K-ATP conductance (Keizer & Magnus, 1989), the difference in the ADP concentration between the silent and active phases of bursting was about 5% (2.0 to 2.1 mM) and the corresponding change in conductance of the K-ATP channel was about 8%, or 30 pS. Thus the data of Smith et al. (1990) cannot rule out this model. Recently Henquin (1990*a*) has provided experimental evidence that suggests periodic modulation of the K-ATP conductance may determine the interburst interval.

Following Keizer and Magnus (1989), the conductance $g_{K\text{-}ATP}$ is assumed to be a function of ATP and ADP concentrations

$$g_{K\text{-}ATP} = \bar{g}_{K\text{-}ATP}\left[\frac{1 + \dfrac{[ADP]}{K_1}}{1 + \dfrac{[ADP]}{K_1} + \dfrac{[ATP]}{K_2}}\right]. \qquad (26)$$

Values for $K_1$ and $K_2$ are derived from Kakei et al. (1986). Equation (25) for $I_{K\text{-}ATP}$ is used. Keizer and Magnus (1989) assumed that the concentrations of ATP and ADP are modulated via inhibition, by $Ca^{2+}$ uptake, of oxidative phosphorylation. This led them to posit the following differential equation

$$\frac{d[ADP]}{dt} = -k\exp\left\{R\left[1 - \frac{[Ca]}{R_1}\right]\right\}[ADP] + k[ATP] \qquad (27)$$

in which $[A] = [ATP] + [ADP]$ is given a constant value.

This mechanism postulates the uptake of cytosolic $Ca^{2+}$ by mitochondria under physiological conditions. Several groups have shown that this occurs in $\beta$-cells, the most recent (Lenzen & Rustenbeck, 1991) in permeabilized ob/ob islets. The uptake of $Ca^{2+}$ into liver mitochondria is known (Lehninger, 1975) to interfere with the chemiosmotic synthesis of ATP. It is this process that provides the $Ca^{2+}$-to-ADP coupling responsible for bistability in the Keizer-Magnus mechanism, a more detailed account of which is in preparation (G. Magnus, *in preparation*[1]). An alternative coupling mechanism has been offered by Henquin (1990*a*), who suggested that $Ca^{2+}$-ATPase pumps could affect the ATP-ADP dynamics in a similar fashion. While this may be so, it seems less likely to us. Indeed, the fixed stoichiometric relationship between ATP and $Ca^{2+}$ for these pumps would not seem to allow for the amplification of a submicromolar change in $Ca^{2+}$ concentration into the submillimolar changes in ATP and ADP concentrations required to affect the K-ATP channels.

We have combined this model with the earlier equations for $Ca^{2+}$ and delayed-rectifier channel currents and $Ca^{2+}$ dynamics to yield a whole-cell model with eight differential equations—Eqs. (5), (13)–(15), (21), (22), (25) and (27). The chief differences between this model and that considered by Keizer and Magnus (1989) are first, the inclusion of the improved model for the $Ca^{2+}$ currents developed in this paper, and second, the faster time scale for [Ca] change in the present model. Thus, [ADP] or $g_{K\text{-}ATP}$, which is a function of [ADP] via Eq. (26), is now the slow variable capable of driving bursting.

In contrast to the slow voltage inactivation model examined in the preceding sections, this model exhibits reasonable Z curves without modification of $Ca^{2+}$ channel parameters. The solution, however, although periodic, does not "burst," but rather exhibits a *complex oscillation between* depolarized and hyperpolarized states. Nonetheless, in this model the Z curve is robust. Thus it is possible to change parameters within the physiological range to modify the position and characteristics of the Z curve and the resulting oscillations. In doing this we

[1] Ph.D. dissertation, Department of Chemistry, University of California, Davis.

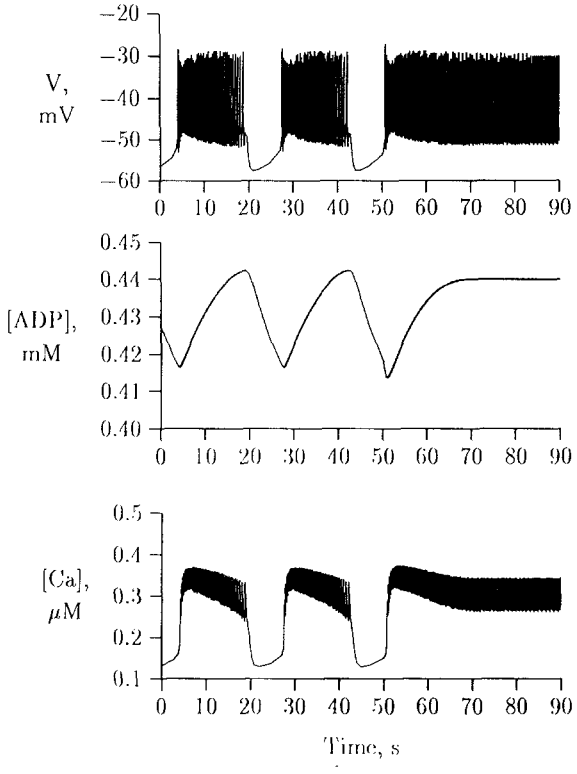


**Fig. 6.** Bursting, with a transition to continuous spiking after 50 sec, as obtained with the revised Keizer-Magnus model containing a modulable K-ATP conductance. Time courses for voltage, [ADP], and [Ca] are shown. All horizontal axes are in seconds.

have found a range of parameters in which bursts like those shown in the left portion of Fig. 6 are obtained. The parameters that yield these bursts are the "standard" values given in the Table with the exception of $\bar{g}_{Ca} = 4116$ pS, $V_{mf} = -15$ mV, $A = 4.234$ mM$^{-1}$ mV$^{-1}$ msec$^{-1}$, and $V_{ns} = -11$ mV. This shift of $-11$ mV does not remove the sharp lower threshold for the $Ca^{2+}$ currents but only moves it close to $-50$ mV, which is similar to the value reported by Rorsman and Trube (1986). It should be noted that the simulation in Fig. 6 employed $I_{CaG}$ (Eq. (24)). Although that current is very small ($g_{CaG} = 17.6$ pS mM$^{-1}$), it is crucial in adjusting the position of the silent phase close to $-58$ mV. In fact, during the silent phase, this small current is equal to the total net current (ca. 1 pA). To achieve electrical activity like that shown in Fig. 6, it is not necessary that this current be carried exclusively by $Ca^{2+}$. Indeed, we have obtained similar bursts by substituting an inward "leak" current, nonspecific as to cation.

Figure 6 illustrates several important features of bursting according to this mechanism. First, by setting the fraction of cytosolic calcium that is free to 0.03, we have been able to make [Ca] a fast variable. [Ca] varies between 0.13 and 0.34 μM. [Ca] exhibits a rapid rise at the beginning of the active phase, a long plateau with superimposed spikes during the active phase, and a somewhat slower fall at the beginning of the silent phase. These features are in good agreement with the observations of Santos et al. (1991). A second feature is the small change in [ADP] during the bursts (ca. 0.025 mM) and the accompanying small change in $g_{K\text{-}ATP}$ (ca. 20 pS). This latter change is less than 10% of the average $g_{K\text{-}ATP}$ (236 pS), which is on the order of the measured $K^+$ conductance in 8 mM glucose (Smith et al., 1990), and well below the 50-pS resolution of Smith et al. (1990).

Another feature of this mechanism is that the parameter $R$ in Eq. (27) reflects the positive effect of the proton motive force on the production of ATP from ADP. Although the equation for metabolism of ATP is quite primitive, it does imply that $R$ should be an *increasing* function of glucose concentration. Thus an increase in $R$ would be expected to lead to continuous spiking, whereas a decrease in $R$ should lead to hyperpolarization. This is indeed the case. Bursting occurs for $0.55 < R < 0.97$, with a hyperpolarized state for lower values and continuous spiking for higher values. In Fig. 6, $R$ has been increased abruptly to 1.4 at $t = 50$ msec, so the last 30 sec of this figure show typical continuous spiking. The continuous voltage spikes closely resemble those seen experimentally, and [Ca] oscillates in synchrony about a physiologically reasonable value of 0.3 μM. Because [Ca] is a fast variable, the amplitude of the oscillations is appreciable (0.04 μM). Since the conductance of the nonspecific cation channel reported by Rojas et al. (1990) increases in the presence of glucose, it is worth noting here that similar bifurcations occur as $g_{CaG}$ is increased.

The detailed characteristics of the voltage bursts are similar to those seen experimentally. Thus the silent phase is at $-58$ mV, the plateau voltage ca. $-50$ mV, and the spikes have an amplitude ca. 22 mV. The period of the bursts, 24 sec in Fig. 6, is, roughly, inversely proportional to the parameter $k$ in Eq. (27). The frequency of the spikes in the active phase decreases from a maximum of about 4 sec$^{-1}$ at the onset to less than 2 sec$^{-1}$ at the end, as is characteristic of β-cells in islets (Cook, Satin & Hopkins, 1991). The shape of the spikes also changes from the beginning to the end of the active phase, with the final spikes developing a small pre-spike "hump" prior to depolarization while retaining a rapid repolarization to the plateau. The average conductance for the delayed rectifier in the plateau region is 20

pS, about 10% that of the K-ATP conductance. The size of the spikes can be adjusted up or down by decreasing or increasing the ratio $\bar{g}_{KV}/\bar{g}_{K\text{-}ATP}$.

It has been conjectured (Cook et al., 1991) that the increase in the interspike interval towards the end of the active phase may be due to slow voltage inactivation of $Ca^{2+}$ currents through the variable $J$. We find no evidence for this from simulations in which the value of $J$ is fixed. The slow decline in the frequency of spikes during the active phase is unchanged by fixing either $I$ or $J$, neither of which have been found to be essential variables in this model. In this model it is the dynamics of the dominant "slow" variable, [ADP], as it interacts with the "fast" variables $V$ and $n$ that determine both the interburst interval and the slowing of the spike frequency at the end of a burst.

## Concluding Remarks

It has been possible to achieve a reasonable fit to the experimental activation and inactivation measurements of Hopkins et al. (1991) using two types of calcium currents, one rapidly inactivated by $Ca^{2+}$ and the other slowly inactivated by voltage. Adding a K-ATP current and a delayed-rectifier $K^+$ current to produce a "whole-cell" model, we have investigated the hypothesis that slow voltage inactivation of a calcium current is sufficient to produce bursting in mouse $\beta$-cells. We have found that this is possible only if the parameters of the $Ca^{2+}$ currents are significantly altered from those that fit the whole-cell recordings. The alterations that are required include: broadening the lower threshold for the $Ca^{2+}$ $I$-$V$ curve, shifting the activation to more negative potentials, and decreasing the slopes of the $Ca^{2+}$ current inactivation curves. Even then, the existence of bursting is confined to a very narrow range of parameters and does not seem robust. Since we have relied on experimental measurements made in the dialyzed whole-cell configuration at room temperature, we cannot rule out that the kinetics of the $Ca^{2+}$ currents are different in intact cells or at the higher temperatures (27–37°C) required for bursting. Our calculations do make it clear, however, that significantly more activation of $Ca^{2+}$ currents in the threshold region ($-55$ to $-45$ mV) would be necessary for slow voltage inactivation to be effective in setting the interburst interval.

In the presence of a K-ATP conductance that can be modulated dynamically by ATP and ADP, less drastic changes in the measured $Ca^{2+}$ currents are required to produce bursting. These include shifting the activation curves by $-11$ mV and adding a small leak current. In this second "whole-cell" model changes in the K-ATP conductance, associated with modulation of the ATP/ADP ratio by $Ca^{2+}$ handling in the mitochondria, are responsible for determining the interburst interval. In this model only a small change in the K-ATP conductance (20 pS) is required to produce bursting—an amount that would be difficult to detect with present experimental techniques (Smith et al., 1990). Cytosolic $Ca^{2+}$ is not required to change slowly in either of our whole-cell models, and its time course appears rather similar to that observed in perfused islets (Santos et al., 1991). Because of the large alterations in the measured $Ca^{2+}$ currents that are required to produce bursting, we are inclined to favor modulation of the K-ATP channel over slow voltage inactivation as a mechanism for determining the interburst interval in mouse $\beta$-cells. Future measurements of $Ca^{2+}$ currents under more physiological conditions, including determination of the residual current that did not inactivate in measurements by Hopkins et al. (1991), will be required to clarify the situation further.

This work was supported in part by NSF grant DIR-90-06104 and the Agricultural Experiment Station of the University of California. P.S. gratefully acknowledges financial support from an NRC Fellowship. We have benefited from numerous conversations with Drs. John Rinzel, Arthur Sherman, Daniel Cook, and Leslie Satin.

## References

Ashcroft, F., Rorsman, P. 1989. Electrophysiology of the pancreatic $\beta$-cell. *Prog. Biophys. Mol. Biol.* **54:**87–143

Ashcroft, S., Smith, P. 1989. Glucose modulates L-type Ca channels in murine isolated pancreatic $\beta$-cells. *J. Physiol.* **417:**79P

Atwater, I., Dawson, C., Scott, A., Eddleston, G., Rojas, E. 1980. Biochemistry and Biophysics of the Pancreatic $\beta$-Cell. George Thieme, New York

Chay, T. 1990. Effect of compartmentalized Ca ions on electrical bursting activity of pancreatic $\beta$-cells. *Am. J. Physiol.* **258:**C955–C965

Chay, T., Keizer, J. 1983. Minimal model for membrane oscillations in the pancreatic $\beta$-cell. *Biophys. J.* **42:**181–190

Cook, D., Ikeuchi, M. 1989. Tolbutamide as mimic of glucose on $\beta$-cell electrical activity, ATP-sensitive $K^+$ channels as common pathway for both stimuli. *Diabetes* **38:**416–421

Cook, D., Satin, L., Hopkins, W. 1991. Pancreatic $\beta$-cells are bursting, but how? *Trends Neurosci.* **14:**411–414

Fatherazi, S., Cook, D.L. 1991. Specificity of tetraethylammonium and quinine for three K channels in insulin-secreting cells. *J. Membrane Biol.* **120:**105–114

Henquin, J. 1990*a*. Glucose-induced electrical activity in $\beta$-cells, feedback control of ATP-sensitive $K^+$ channels by $Ca^{2+}$. *Diabetes* **39:**1457–1460

Henquin, J. 1990*b*. Role of voltage- and $Ca^{2+}$-dependent $K^+$ channels in the control of glucose-induced electrical activity in pancreatic $\beta$-cells. *Pfluegers Arch.* **416:**568–572

Hopkins, W., Satin, L.S., Cook, D.L. 1991. Inactivation kinetics

and pharmacology distinguish two calcium currents in mouse pancreatic β-cells. *J. Membrane Biol.* **119:**229–239

Kakei, M., Kelly, R., Ashcroft, S., Ashcroft, S. 1986. The ATP-sensitivity of $K^+$ channels in rat pancreatic β-cells is modulated by ADP. *FEBS Lett.* **208:**63–66

Keizer, J., Magnus, G. 1989. ATP-sensitive potassium channels and bursting in the pancreatic β-cell. *Biophys. J.* **56:**229–242

Keizer, J., Smolen, P. 1991. Bursting electrical activity in pancreatic beta cells caused by $Ca^{2+}$-and voltage-inactivated $Ca^{2+}$ channels. *Proc. Natl. Acad. Sci. USA* **88:**3897–3901

Kukuljan, M., Goncalves, A.A., Atwater, I. 1991. Charybdotoxin-sensitive $K_{Ca}$ channel is not involved in glucose-induced electrical activity in pancreatic β-cells. *J. Membrane Biol.* **119:**187–195

Lehninger, A. 1975. Biochemistry. pp. 531–533. Worth, New York

Lenzen, S., Rustenbeck, I. 1991. Effects of $IP_3$, spermine, and $Mg^{2+}$ on regulation of $Ca^{2+}$ transport by endoplasmic reticulum and mitochondria in permeabilized pancreatic islets. *Diabetes* **40:**323–326

Malecot, C., Feindt, P., Trautwein, W. 1988. Intracellular N-methyl-D-glucamine modifies the kinetics and voltage-dependence of the calcium current in guinea pig ventricular heart cells. *Pfluegers Arch.* **411:**235–242

Misler, S., Falke, L., Gillis, K., McDaniel, M. 1986. A metabolite-regulated channel in rat pancreatic β-cells. *Proc. Natl. Acad. Sci. USA* **83:**7119–7123

Misler, S., Gee, W., Gillis, K., Scharp, D., Falke, L. 1989. Metabolite-regulated ATP-sensitive $K^+$ channels in human pancreatic islet cells. *Diabetes* **38:**422–427

Plant, T. 1988. Properties and calcium-dependent inactivation of calcium currents in cultured mouse pancreatic β-cells, *J. Physiol.* **404:**731–747

Rinzel, J. 1985. Bursting oscillations in an excitable membrane model. *In*: Ordinary and Partial Differential Equations. B. Sleeman and R. Jarvis, editors. pp. 304–316. Springer-Verlag, New York

Rojas, E., Hidalgo, J., Carroll, P., Li, M., Atwater, I. 1990. A new class of calcium channels activated by glucose in human pancreatic β-cells. *FEBS Lett.* **261:**265–270

Rorsman, P., Trube, G. 1986. Calcium and delayed potassium currents in mouse pancreatic β-cells under voltage-clamp conditions. *J. Physiol.* **374:**531–550

Santos, R., Rosario, L., Nadal, A., Garcia-Sancho, J., Soria, B., Valdeolmillos, M. 1991. Widespread synchronous $Ca^{2+}$ oscillations due to bursting electrical activity in single pancreatic islets. *Pfluegers Arch.* **418:**417–422

Satin, L., Cook, D. 1988. Evidence for two calcium currents in insulin-secreting cells. *Pfluegers Arch.* **411:**401–409

Satin, L., Cook, D. 1989. Calcium current inactivation in insulin-secreting cells is mediated by calcium influx and membrane depolarization. *Pfluegers Arch.* **414:**1–10

Sherman, A., Keizer, J., Rinzel, J. 1990. Domain model for $Ca^{2+}$-inactivation of $Ca^{2+}$ channels at low channel density. *Biophys. J.* **58:**985–995

Sherman, A., Rinzel, J., Keizer, J. 1988. Emergence of organized bursting in clusters of pancreatic β-cells by channel sharing. *Biophys. J.* **54:**411–425

Smith, P., Ashcroft, F., Rorsman, P. 1990. Simultaneous recordings of glucose dependent electrical activity and ATP-regulated $K^+$-currents in isolated mouse pancreatic β-cells. *FEBS Lett.* **261:**187–190

Valdeolmillos, M., Santos, R., Contreras, D., Soria, B., Rosario, L. 1989. Glucose-induced oscillations of intracellular $Ca^{2+}$ concentration resembling bursting electrical activity in single mouse islets of Langerhans. *FEBS Lett.* **259:**19–23

Received 6 June 1991; revised 30 October 1991